Journal of Catalysis **203,** 257–263 (2001)
doi:10.1006/jcat.2001.3330, available online at http://www.idealibrary.com on IDEAL®

The Inhibiting Effect of Lanthanum on the Formation of Benzene over $PtSn/Al_2O_3$ Reforming Catalysts

G. Del Angel,*,[1] A. Bonilla,* J. Navarrete,† E. G. Figueroa,† and J. L. G. Fierro‡

*Universidad Autónoma Metropolitana-Iztapalapa, Departamento de Química, P.O. Box 55-534, C.P. 09340 Mexico, D.F., Mexico; †Instituto Mexicano del Petróleo, Eje Central Lázaro Cárdenas 152, A.P. 14-805, C.P. 07730, Mexico, D.F., Mexico; and ‡Instituto de Catálisis y Petroleoquímica, CSIC, Cantoblanco, 28049 Madrid, Spain

Received October 13, 2000; accepted July 1, 2001

The effect of La_2O_3 on the catalytic properties of $PtSn/Al_2O_3$ reforming catalysts has been investigated. On catalysts with low La_2O_3 content (1 wt%) FTIR CO adsorption spectra show two absorption bands at 2070 and 2122 cm^{-1}. At higher La_2O_3 content (20 wt%) the band at 2070 cm^{-1} diminishes progressively until it completely disappears, while the band at 2122 cm^{-1} increases and shifts to 2130 cm^{-1}. This band is assigned to CO adsorbed on oxidized Pt. This effect is observed on samples on which $PtSn–La_2O_3$ multiphase coexists. The presence of Pt in an oxidized state is supported by XPS since Pt^{2+} is present on the catalysts containing Pt/Sn and La_2O_3. On the other hand, XPS revealed the presence of Sn^{2+} and Sn°. For the *n*-heptane reaction the selectivity pattern of the $PtSn/Al_2O_3$–La catalysts shows total inhibition of the formation of benzene, high olefin content, and low *n*-C_7 dehydrocyclization products.

Key Words: **PtSn catalysts; reforming catalysts; lanthanum effect; *n*-heptane dehydrocyclization.**

INTRODUCTION

The platinum–tin–alumina-supported catalysts were widely used in the petroleum industry for naphtha reforming. The advantage of these catalysts over monometallic platinum catalysts is that they provide increased selectivity to high octane products and better resistance to coke deactivation (1). Important progress in the modification of the bimetallic phase in catalysts has been made and reported in a large number of papers (2–5). Research has been focused on the effect of the Sn oxidation state in the activity and selectivity of Pt for the production of high octane gasoline. However, the continuing requirement for pollution control demands gasoline with low content of aromatics and more isomerized hydrocarbons.

The effect of lanthanides on alumina support is mainly related to the thermal stabilization of the alumina substrate (6–9). Recent studies, however, do not restrict lanthanide effects to the magnification of the textural properties of the support. It has been reported that lanthanides strongly modify the TPR profiles of supported noble metals (10, 11). It has also been shown that lanthanides improve the Lewis acidity of aluminas (12).

As is well known, reforming is a bifunctional reaction where the support acidity plays an important role in the isomerization/dehydrocyclization of hydrocarbons.

Despite its importance to the activity and selectivity properties of reforming reactions, modification of the support has received less attention. Since lanthanides modify the reduction behavior of noble metals, it will be interesting to study this effect in bimetallic PtSn/alumina reforming catalysts. These catalysts are interesting since a large stabilization of tin oxide can be expected and thus the PtSn alloy formation that has been reported by several authors (13–16) would be highly inhibited. Since the lanthanides are usually added to the alumina by impregnation of the support, we can expect an additional effect on the platinum–tin cluster when it is covered with lanthanum oxide. To avoid this phenomenon, in the present work we have prepared $PtSn/Al_2O_3–La_2O_3$ reforming catalysts by adding the lanthanum precursor to boehmite, since in this way the lanthanum will be integrated with the support.

The support prepared by this method was first stabilized by thermal treatment and then impregnated with the metallic precursors. The catalyst was characterized by FTIR CO adsorption, XPS, TEM, and the catalytic activities in the cyclohexane dehydrogenation and *n*-heptane dehydrocyclization reactions.

EXPERIMENTAL

Preparation of Catalysts

Supports. The Al_2O_3 reference support was prepared by direct calcination of Catapal B Boehmite in air at 500°C. The Al_2O_3–La supports were obtained by impregnation of boehmite Catapal B with aqueous solutions of $La(NO_3)_3 \cdot 6H_2O$ to obtain 1, 10, and 20 wt% La. After

[1] To whom correspondence should be addressed. Fax: 52 5 804 46 66. E-mail: gdam@xanum.uam.mx.

0021-9517/01 $35.00

TABLE 1

Catalysts Characterization Data

Catalyst	Pt (wt%)[a]	Sn (wt%)[a]	Pt (wt%)[b]	Sn (wt%)[b]	Cl (wt%)[c]	D (%)[d]	Particle size (Å) Chem[d]	Particle size (Å) TEM[e]
Pt/A	0.56	—	0.49	—	0.39	52	19	18
Pt/A–La20	0.33	—	0.35	—	0.59	57	17	13
PtSn/A	0.53	0.15	0.45	0.10	0.45	—	—	16
PtSn/A–La1	0.44	0.47	0.24	0.36	0.61	—	—	26
PtSn/A–La10	0.2	0.39	0.2	0.38	4.1	—	—	20
PtSn/A–La20	0.38	0.45	0.21	0.47	4.13	—	—	16

[a] Determined by atomic absorption spectroscopy.
[b] Plasma spectroscopy.
[c] Determined by volumetry.
[d] Determined by CO chemisorption.
[e] Determined by TEM (transmission electron microscopy).

impregnation, the Al_2O_3–La supports were calcined in an air stream at 650°C. The surface-specific area of the Al_2O_3 substrate was 221 $m^2\ g^{-1}$, while the surface areas of Al_2O_3–La1, Al_2O_3–La10, and Al_2O_3–La20 were 171, 170, and 112 $m^2\ g^{-1}$, respectively.

Catalysts. A reference Pt catalyst was prepared by wet impregnation of the Al_2O_3 support with a solution of $H_2PtCl_6 \cdot 6H_2O$ in 0.1 M HCl. The PtSn bimetallic catalysts were prepared by coimpregnation of the Al_2O_3 and Al_2O_3–La supports using solutions of $H_2PtCl_6 \cdot 6H_2O$ and $SnCl_4 \cdot 5H_2O$. The nominal contents of Pt and Sn were 0.5 and 0.3 wt%, respectively. The solids were dried at 120°C for 12 h and then calcined in air flow (3.6 l h^{-1}) at 500°C for 4 h; finally the samples were reduced under hydrogen flow (3.6 l h^{-1}) at 500°C for 4 h. The Pt and Sn contents on PtSn catalysts were determined by atomic absorption and plasma spectroscopies. The chloride amount was determined by a volumetric method (Table 1).

Chemisorption

CO chemisorption was carried out in a conventional gravimetric apparatus, producing a dynamic vacuum. Samples (300 mg) were reduced under a hydrogen stream for 1 h at 400°C and then outgassed at the same temperature. The CO chemisorption was determined by introducing CO into the gravimetric system at 70°C and a pressure of 100 Torr. CO irreversibly adsorbed was calculated from values obtained after evacuation of the sample for 1 h at the same temperature. The number of active sites was calculated assuming a stoichiometric CO/Pt ratio equal to one (17, 18). Results were expressed as percentages of metallic dispersion (D%).

Transmission Electron Microscopy

Mean particle size was determined by TEM using a JEOL 100CX apparatus. There were counted approximately 500 particles per sample. The histograms showed a monodistribution of the particle size. The mean particle size d_s was determined using the equation $d_s = \Sigma n_i d_i^3 / \Sigma n_i d_i^2$ (where n_i is the number of particles with diameter d_i).

FTIR Experiments

The FTIR study was carried out at room temperature using a Nicolet-FX710 apparatus. The samples, pressed into thin wafers, were placed in a Pyrex glass cell equipped with CaF_2 windows. The samples were activated *in situ* at 400°C for 30 min under vacuum (10^{-6} Torr). CO admission was carried out at 200°C and 20 Torr; afterward the cell was cooled to room temperature, excess CO was evacuated over 30 min, and then the CO spectra were recorded.

XPS Measurements

The XPS studies were recorded using a VR Escalab 200R electron spectrometer equipped with a hemispherical analyzer, operating in a constant pass energy mode, and a nonmonochromatized Mg$K\alpha$ ($h\nu = 1253.6$ eV, 1 eV $= 1.603 \times 10^{-19}$ J) X-ray source operated at 10 mA and 12 kV. A PDP 11/04 computer (Digital Co.) was used to record and analyze the spectra. All samples were reduced *in situ* under hydrogen at 300°C for 1 h. The intensities of the peaks were estimated by calculating the integral of each peak after subtracting an S-shaped background and fitting the experimental peak to a combination of Lorentzian/Gaussian lines of variable proportions. The binding energies (BE) were referenced to the Al 2p peak, the BE of which was fixed at 74.5 eV.

Catalytic Activity

The activity for the cyclohexane dehydrogenation was carried out in a conventional flow reactor used in the differential mode at low conversion (<15%). Reactants were cyclohexane from Aldrich and UHP hydrogen. Reaction conditions were partial pressure of cyclohexane and hydrogen, 48.2 and 711.8 Torr, respectively; catalyst mass, 0.010–0.050 g; and reaction temperature, 300°C. The *n*-heptane conversion was determined in a conventional flow reactor used in the differential mode at low conversion (<15%). Reactants were *n*-heptane from Merck and UHP hydrogen from AGA. Reaction conditions were partial pressure of *n*-heptane and hydrogen, 11 and 749 Torr, respectively; catalyst mass, 0.050 g; and reaction temperature, 490°C. Hydrogen saturated with *n*-heptane was admitted through the reactor, the products were analyzed by on-line gas chromatography. The column used was a crosslinked methyl siloxane of 50 m × 0.2 mm × 0.5 μm. The products were identified with a HP-GC-MS 5973 gas chromatograph mass spectrometer.

RESULTS

Pt, Sn, and Chloride Content

Using atomic absorption or plasma spectroscopy, good agreement was found between nominal and evaluated platinum content for Pt/A and PtSn/A catalysts. In catalysts containing lanthanum the platinum content was lower than the attained content (Table 1). The presence of lanthanum on Pt/A catalysts greatly interfered with the estimation of the Pt content. On the other hand, the chloride content dramatically increased to unexpected values when lanthanum and tin coexisted on the catalysts. Chloride contents of 4.1 and 4.13 wt% were obtained for catalysts at 10 and 20 wt% La, respectively.

Characterization of the Metallic Phase

The mean particle sizes obtained from electron microscopy and calculated from the expression $d_s = \Sigma n_i d_i^3 / \Sigma n_i d_i^2$ for the various catalysts are reported in Table 1. Mean particle sizes between 13 and 26 Å were obtained. Unimodal particle size distribution for all catalysts was observed in all cases. Particle size distributions for two selected catalysts are shown in Fig. 1. To corroborate the validity of the electron microscopy results, particle size in the Pt/A and Pt/A–La20 samples was determined by CO chemisorption. The values obtained from the two methods were compared and reasonably good agreement was observed.

Additionally, the metallic phase was also determined by the catalyst reactivity in the cyclohexane aromatization. This indirect method is recommended when lanthanides coexist with supported platinum on alumina (19). The specific rates for cyclohexane aromatization are reported in Table 2. The values are given in mol s^{-1} g_{cat}^{-1} and mol s^{-1} g_{Pt}^{-1}.

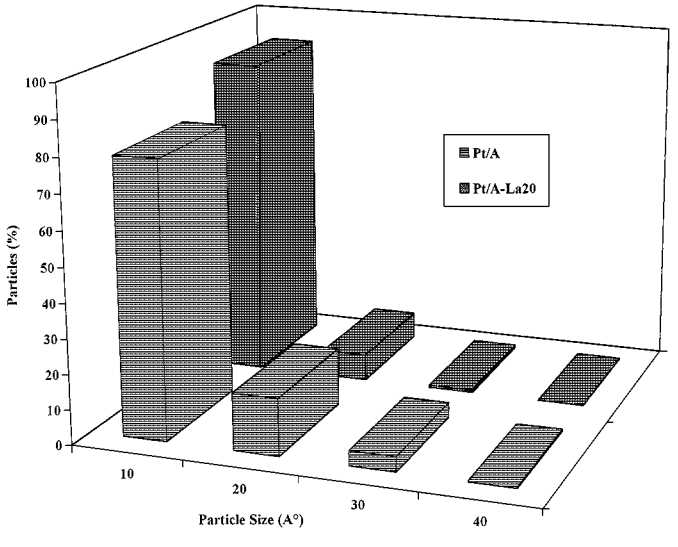

FIG. 1. Particle size distribution for Pt/A and Pt/A–La20 catalysts.

TABLE 2

Catalytic Activities for Cyclohexane Dehydrogenation Reaction over Pt and PtSn Supported on Alumina and Alumina Modified with La

Catalyst	Rate × 10^6 (mol s^{-1} g_{cat}^{-1})	Rate × 10^2 (mol s^{-1} g_{Pt}^{-1})
Pt/A	117.0	2.0
Pt/A–La20	66.0	2.0
PtSn/A	108.0	2.0
PtSn/A–La1	9.82	0.2
PtSn/A–La10	0.53	0.026
PtSn/A–La20	0.04	0.001

The Pt/A, Pt/A–La20, and PtSn/A catalysts were the catalysts showing the highest activity. However, an important effect on the activity was observed when platinum, tin, and lanthanum coexisted: the activity diminished by a factor of about 10^{-3} as can be seen in Table 2 for the PtSn/A–La20 catalyst. Therefore, an important difference in metal accessibility is obtained by the coimpregnation of Sn and Pt on a lanthanum-doped alumina substrate.

CO Chemisorption by FTIR

The IR spectra of CO chemisorbed on the Pt- and PtSn-supported catalysts are shown in Figs. 2 and 3. The infrared spectrum for Pt/A showed a main peak at 2067 cm^{-1} and a

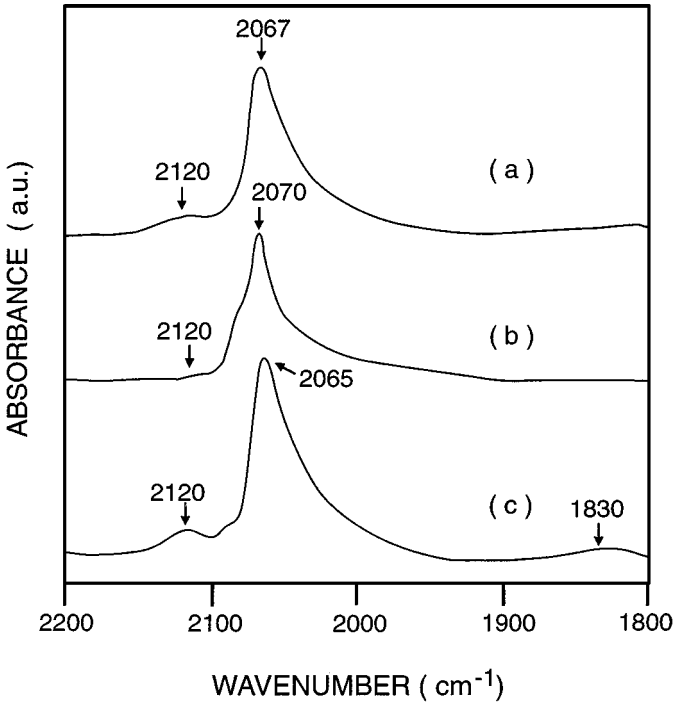

FIG. 2. Infrared spectra of CO chemisorbed on different catalysts: (a) Pt/A, (b) Pt/A–La20, and (c) PtSn/A.

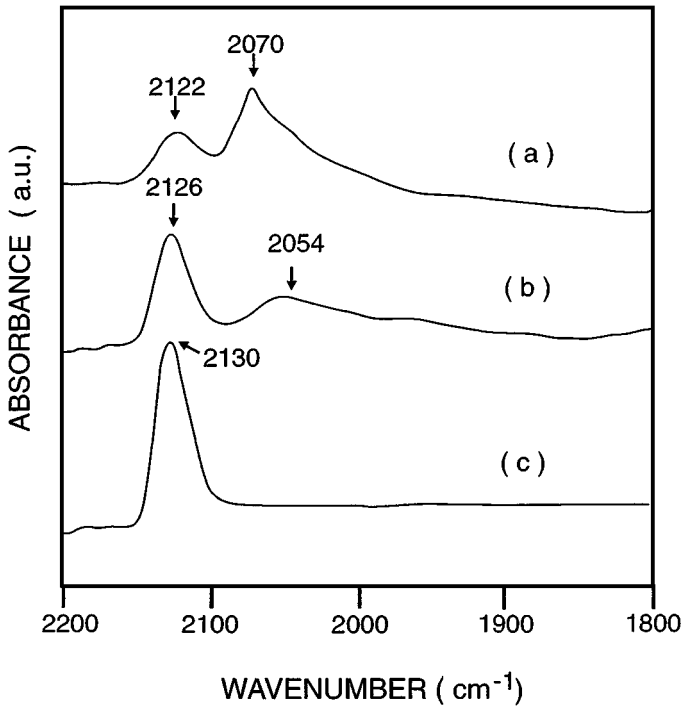

FIG. 3. Infrared spectra of CO chemisorbed on different catalysts: (a) PtSn/A–La1, (b) PtSn/A–La10, and (c) PtSn/A–La20.

very low signal at 2120 cm^{-1} (Fig. 2). The main band at 2067 cm^{-1} is assigned to linearly adsorbed CO and related to the CO adsorbed on the edge atoms (20). The band at 2120 cm^{-1} is assigned to chloride effects (21). The band at 1830 cm^{-1} corresponding to bridged CO adsorption is not observed in the present catalysts. The Pt monometallic catalyst supported on the alumina with 20% lanthanum (Pt/A–La20) and the bimetallic PtSn supported on alumina (PtSn/A) showed spectra similar to those of the Pt/A catalyst, bands at 2070 and 2120 cm^{-1} for the former and bands at 2065 and 2120 cm^{-1} for the latter. The bimetallic PtSn catalyst supported on alumina doped with 1 wt% La (PtSn/A–La1) shows a decrease in the intensity of the main peak at 2070 cm^{-1} and the band at higher frequency shows a slight shift to 2122 cm^{-1} (Fig. 3). The PtSn samples supported on lanthanum-doped alumina show progressive decrease of the main peak for the catalyst at 10% La, until its disappearance in the 20% La catalyst. The catalyst PtSn/A–La10 presents a wide peak at 2054 cm^{-1} and the second peak increases and shifts to a high frequency of 2126 cm^{-1}, whereas in the PtSn/A–La20 catalyst only the latter band appears and it is shifted to 2130 cm^{-1}.

X-Ray Photoelectron Spectroscopy

Binding energies of core electrons and surface atomic ratios of Pt and Pt–Sn catalysts are reported in Tables 3 and 4 (see Figs. 4 and 5). The binding energy Pt4$d_{5/2}$ for Pt/A–La20 and PtSn/A samples indicates that Pt is present as Pt^0 but in a very dispersed state, particularly in the sample with La (higher Pt/Al atomic ratio, Table 4). However, when Pt and Sn are impregnated on the lanthanum–alumina support the binding energy of the Pt4$d_{5/2}$ peak decreases around 1 eV and the percentage of the area decreases as the La content increases (100% in PtSn/A–La1, 58% in PtSn/A–La10, and 53% for PtSn/A–La20; Fig. 4). A second Pt component is observed at higher binding energies (316.9 and 317.3 eV) corresponding to an oxidized species of Pt (Pt^{2+}), for PtSn/A–La10 and PtSn/A–La20. For the catalysts with Sn, the peak Sn3$d_{5/2}$ presents two components, shown as a percentage of each peak in Table 3. One minor low-binding-energy component (483.9 eV for PtSn/A and up to 484.7 eV for PtSn/A–La1 and PtSn/A–La10) can be associated with a reduced phase (as Sn^0 or one alloyed phase $SnPt_x$). Another major component (higher at 81% and close to 487 eV) is characteristic of the Sn oxidized species Sn^{2+}. Binding energy Sn3$d_{5/2}$ around 488 eV, corresponding to Sn^{+4}, is not observed in the XPS spectra.

In Table 3 the binding energies of La3$d_{5/2}$ of the La content catalysts are reported. It can be seen that the values of 835, 834.9, and 835.2 eV are close to the value corresponding to La_2O_3 (834.92 eV, La^{3+}); therefore, we can assume that platinum does not reduce the lanthanum oxide. Note that the reported values correspond to those obtained on samples reduced *in situ* with H_2.

TABLE 3

Binding Energies (eV) of Core Electrons of Pt3$d_{5/2}$ in Pt and PtSn Supported Catalysts

Catalyst	Pt4$d_{5/2}$	Sn3$d_{5/2}$	Al2p	La3$d_{5/2}$
Pt/A–La20	316	—	74.5	835
PtSn/A	316.1	483.9 (19)	74.5	—
		487.3 (81)		
PtSn/A–La1	315.4	484.7 (9)	74.5	Traces
		487.2 (91)		
PtSn/A–La10	314.7 (58)	484.7 (11)	74.5	834.9
	316.9 (42)	486.7 (89)		
PtSn/A–La20	315.0 (53)	484.4 (16)	74.5	835.2
	317.3 (47)	487.0 (84)		

TABLE 4

Atomic Surface Ratios of Supported Pt and PtSn Catalysts

Catalyst	Sn/Al	Pt/Al	La/Al
Pt/A–La20	—	0.0038	0.063
PtSn/A	0.012	0.0010	—
PtSn/A–La1	0.016	0.0004	Traces
PtSn/A–La10	0.031	0.0011	0.004
PtSn/A–La20	0.011	0.0011	0.049

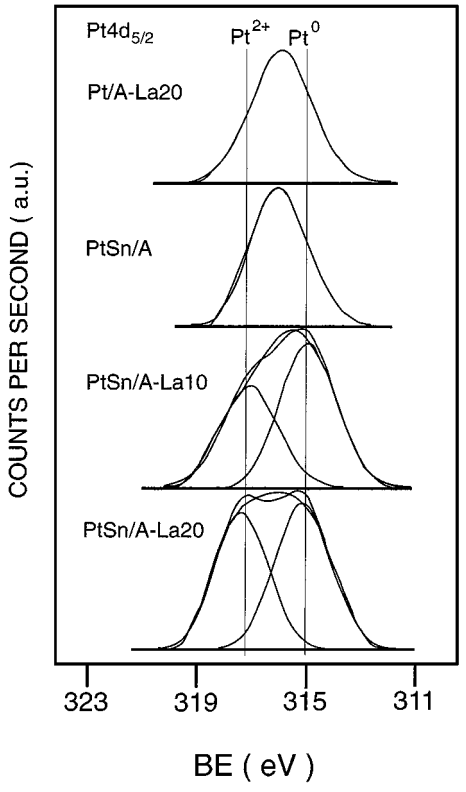

FIG. 4. Pt4$d_{5/2}$ core level spectra of Pt/A–La20, PtSn/A, PtSn/A–La10, and PtSn/A–La20 catalysts.

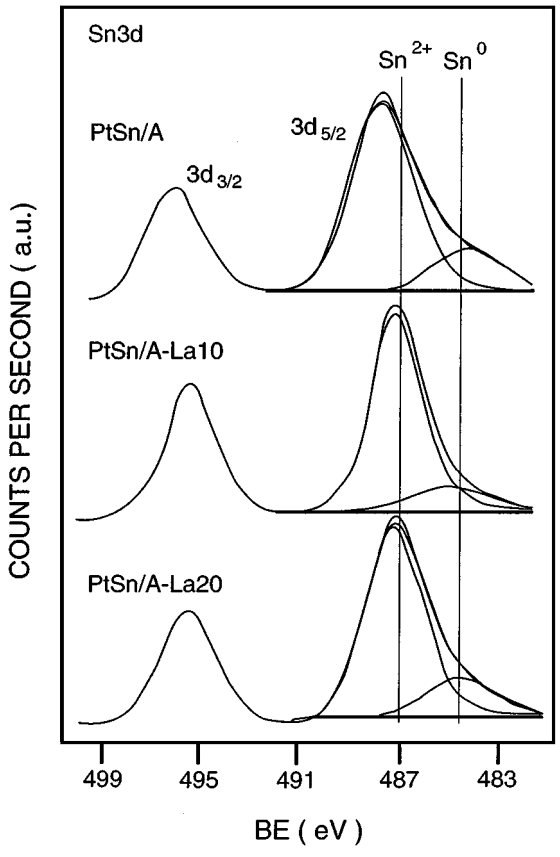

FIG. 5. Sn3*d* core level spectra of PtSn/A, PtSn/A–La10, and PtSn/A–La20 catalysts.

Catalytic Activity

The activity and selectivity for the *n*-heptane reaction in the presence of Pt and PtSn catalysts supported on alumina and lanthanum-doped alumina are shown in Table 5. The activity (rate) of the monometallic Pt catalyst decreases notably in lanthanum-doped alumina supports. It changes from 21 to 1.4×10^{-6} mol s^{-1} g_{cat}^{-1} and from 3.7 to 0.42×10^{-3} mol s^{-1} g_{Pt}^{-1} for Pt/A and Pt/A–La20, respectively. Addition of Sn to Pt supported on alumina (PtSn/A) shows only a slight decrease in activity when compared with the Pt/A catalyst. However, for PtSn catalysts supported on lanthanum-modified alumina, the activity decreases progressively as the La contents increase. These catalysts show activities of 6.2, 0.82, and 0.2×10^{-6} mol s^{-1} g_{cat}^{-1} and 1.4, 0.43, and 0.05×10^{-3} mol s^{-1} g_{Pt}^{-1} for La contents of 1, 10, and 20 wt%, respectively. The selectivity pattern of the products is reported in Table 6. It can be observed that lanthanum strongly modifies the selectivity. In PtSn/A–La10 and PtSn/A–La20 catalysts the selectivity to olefins was increased, whereas the aromatization was substantially suppressed.

DISCUSSION

In Table 1, an excess of chloride content was observed on the catalysts containing high rare earth content; this could be due to the preparation conditions. The metallic precursors were $H_2PtCl_6 \cdot 6H_2O$ and $SnCl_4 \cdot 5H_2O$ in 0.1 M acid solutions. We have then solutions with high chloride content. Under such conditions the excess chlorine can be trapped by the rare earth. The chlorine trapping phenomenon on Pd/Al_2O_3 lanthanum- and cerium-doped catalysts has recently been reported by Kili and Le Normand (22).

In noble metal-supported catalysts the metallic surface area is an important characterization parameter. Classical

TABLE 5

Activity for *n*-Heptane Conversion on Pt and PtSn Supported on Al_2O_3 Modified by La

Catalyst	Rate $\times 10^6$ (mol s^{-1} g_{cat}^{-1})	Rate $\times 10^3$ (mol s^{-1} g_{Pt}^{-1})
Pt/A	21.0	3.7
Pt/A–La20	1.4	0.42
PtSn/A	17.0	3.2
PtSn/A–La1	6.2	1.4
PtSn/A–La10	0.82	0.43
PtSn/A–La20	0.20	0.05

TABLE 6

Selectivity for *n*-Heptane Conversion on Pt and PtSn Supported on Al_2O_3 Modified by La

Catalyst	Selectivity (%)				
	C_1–C_6[a]	Benzene	iC_7[b]	$C_7^=$[c]	Toluene
Pt/A	25.5	1.8	18.3	31	23.2
Pt/A–La20	16.2	5.0	5.1	50.3	23.3
PtSn/A	22.2	2.9	16.8	30.3	27.8
PtSn/A–La1	25.8	0.0	10.4	27.2	36.1
PtSn/A–La10	31.4	0.0	10.0	49.4	9.1
PtSn/A–La20	33.3	0.0	10.3	49.4	7.0

[a] C_1–C_6, C_1 to C_6 hydrocarbons.
[b] iC_7, C_7 isomers.
[c] $C_7^=$, C_7 olefins.

methods based on the measurement of the amount of irreversibly chemisorbed hydrogen and subsequent titration by gaseous hydrogen of the oxygen uptake are generally used to determine the number of active sites on the metal surface. In doped alumina containing lanthanum or cerium oxides, the specific areas of Pd, Rh, and Pt have also been determined by hydrogen chemisorption (10, 19, 23). However, it has been recommended for rare earth–alumina-supported metal catalysts that the metallic surface area be determined by means of the activity in a "structure-insensitive reaction." Benzene hydrogenation and cyclohexane dehydrogenation are classified as structure-insensitive reactions and have been reported to be useful for indirect determination of the metallic surface area (19, 23). In the present work the cyclohexane dehydrogenation activity was taken as a comparative parameter for the determination of the accessible metal area. The monometallic platinum reference catalyst Pt/A showed cyclohexane dehydrogenation activity similar to that of PtSn/A and Pt/A–La20 catalysts (Table 2). The effect of La on the cyclohexane dehydrogenation became important when the three components Pt, Sn, and La coexisted. Cyclohexane dehydrogenation activity is strongly dependent on La content.

IR spectroscopic studies of CO adsorption were used to reveal the nature of the metal surface sites in reduced catalysts. No change in the position of the IR bands at around 2120 and 2070 cm^{-1} for CO adsorption on Pt (Pt/A) was observed when the alumina support was modified by La (Pt/A–La20) or even when the Sn was added to the platinum (PtSn/A; Fig. 2). The infrared band at 2120 cm^{-1} has been associated with CO chemisorbed on a Pt atom surrounded by chloride species, where the platinum is in an oxidized state (24, 25). This is explained on the basis of the electron back donation $d\pi \rightarrow 2\pi^*$ from the metal to the $2\pi^*$ antibonding orbitals of the chemisorbed CO molecules; the stretching frequency of the carbonyl group shifts to higher values and approaches that of gaseous CO frequencies (21). When alumina is doped with La in PtSn catalysts the 2120-cm^{-1} band acquires great importance (Fig. 3).

The presence of Pt in an oxidized state in different amounts, depending on the catalyst composition, is supported by the XPS results. In Table 3 the estimate of the Pt and Pt^{2+} oxidation state is higher for the catalysts in which Pt, Sn, and La coexist. The amount of Pt in a highly oxidized state observed by XPS follows the same trend observed in the behavior of the CO absorption band at 2120 cm^{-1}, since it increases with higher La content (Fig. 4). On the other hand, we can say that PtSn alloys are only formed in small quantities. From the data compiled in Table 3, the presence of Sn^0 is lower than 16% in the PtSn/A–La20 catalyst, whereas most of the tin remains in the oxidized state (Sn^{2+}). Therefore, the band at 2120 cm^{-1} should not be associated with PtSn alloys or in any case its contribution to the band shift is very small. Lanthanum also seems to play a negligible role in the existence of platinum in an oxidized state. In the Pt/A–La20 catalyst, nonoxidized platinum is detected by XPS. In fact, results are surprising when platinum appears as Pt^{2+} in significant amounts, as occurs when Pt, SnO_2, and La_2O_3 coexist. Multiple interaction between the three components seems to be responsible for the stabilization of Pt in its oxidized state. The Pt^0/Pt^{2+} ratio calculated from XPS in PtSn/A–La10 and PtSn/A–La20 catalysts should certainly affect the catalytic activities of cyclohexane dehydrogenation and *n*-heptane dehydrocyclization.

In the catalyst containing 20% La (PtSn/A–La20), the cyclohexane dehydrogenation diminishes by an order of 10^{-3} with respect to the Pt/A catalyst; the rate is expressed in mol s^{-1} g_{cat}^{-1} or in mol s^{-1} g_{Pt}^{-1} (Table 2). Assuming that XPS is a surface-sensitive technique, the possibility of platinum particles being covered by a La_2O_3 layer should be discarded, because the Pt/Al ratio is of the same order (0.0011) as that obtained in sample PtSn/A (0.0010) (Table 4). Thus the accessibility of Pt determined by means of the cyclohexane dehydrogenation rate is rather a tool for the determination of the "active" Pt atoms and these are strongly affected by the multiple Pt–SnO_2–La_2O_3 interactions (Table 2). The role of chlorine in the aromatization of cyclohexane seems to be limited to a chlorination effect of La_2O_3 (22). Even if comparable chlorine contents exist in PtSn/A–La10 and PtSn/A–La20 catalysts, the activities are very different. Moreover, when the PtSn/A catalyst is compared with the PtSn/A–La1 catalyst, both showing chlorine contents of the same order (0.45 and 0.61%), the activities are quite different, 108×10^{-6} vs 9.82×10^{-6} mol sec^{-1} g_{cat}^{-1}. Activity similar to that obtained for cyclohexane dehydrogenation is observed in *n*-heptane conversion (Table 5). The activity decay from Pt/A to PtSn/A–La20 catalysts is on the order of 10^{-2}. Again the effect of the multiple phase interaction is present, although the

analysis of the selectivity pattern in this reaction needs to be considered (Table 6). In the catalysts in which the three components coexist the following was observed: (i) the formation of benzene was suppressed; (ii) the olefins produced increased from 27.2 to 49.4%; and (iii) the *n*-heptane dehydrocyclization diminished from 36.1 to 7.0%. Assuming that substantial proportion of platinum exists in an oxidized state in these catalysts, we can say that the "metallic" character of Pt is inhibited. In a recent work (26) on the *n*-heptane dehydrocyclization reaction it is reported that benzene is a product arising from toluene dealkylation. On the other hand, dealkylation is reported as an essentially "metallic" reaction. Thus inhibition of benzene formation could be due to a diminution of the metallic character of platinum. To be consistent with this assumption the formation of significant amounts of $C_7^=$ can be due to the same effect, i.e., the loss of the metallic character of platinum. The diminution in toluene formation can also be explained with similar arguments. These results appear to be of great importance for the design of reforming catalysts. As it has been clearly demonstrated, the catalyst PtSn/A–La1 showed acceptable activity and good selectivity to toluene, and, most important, it allowed benzene-free reforming products.

CONCLUSIONS

In alumina-supported bimetallic PtSn catalysts doped with lanthanum, the interaction of Pt in the multiple phase Pt–SnO_2–La_2O_3 was revealed. FTIR CO absorption spectra showed two adsorption bands at 2070 and 2122 cm^{-1} on catalysts at low La content. At higher La contents, on PtSn catalysts the band at 2122 cm^{-1} assigned to Pt^{2+} increased and shifted to 2130 cm^{-1}. The XPS spectroscopy studies confirmed the IR results, since the formation of Pt^{2+} was detected. Thus the metallic character of platinum is diminished and its hydrogenation–dehydrogenation properties are affected. For *n*-heptane dehydrocyclization total inhibition of benzene, high olefin content, and low *n*-heptane dehydrocyclization were obtained.

ACKNOWLEDGMENTS

We acknowledge CONACYT for the support provided under Project 4132PE and the Instituto Mexicano del Petróleo for the IMP-FIES Project 96-30-III. A.B. thanks CONACYT for the grant awarded to her.

REFERENCES

1. Rausch, R. E., U.S. Patent 3 745 112, 1973.
2. Srinivasan, R., and Davis, B. H., *Platinum Met. Rev.* **36**, 151 (1992).
3. Kluksdahl, M. E., U.S. Patent 3 415 737, 1968.
4. Martino, G., Miguel, J., and Duhaut, P., French Patent 2 234 924, 1975.
5. Sinfelt, H., U.S. Patent 3 953 368, 1976.
6. Schaper, H., Doesburg, E. B. M., and Van Reijen, L. L., *Appl. Catal.* **7**, 211 (1983).
7. Oudet, F., Vejux, A., and Courtine, P., *Appl. Catal.* **50**, 79 (1989).
8. Beguin, B., Garbowski, E., and Primet, M., *Appl. Catal.* **75**, 119 (1991).
9. Bettman, M., Chase, R. E., Otto, K., and Weber, W. H., *J. Catal.* **117**, 447 (1989).
10. Fuentes, S., Bogdanchikova, N. E., Diaz, G., Peraaza, M., and Sandoval, G. C., *Catal Lett.* **47**, 27 (1997).
11. Pieck, J. S., and Bell, A. T., *J. Catal.* **96**, 88 (1985).
12. Monterra, C., and Magnacca, G., *J. Chem. Soc. Faraday Trans.* **92(4)**, 5111 (1996).
13. Srinivasan, R., Rice, L. A., and Davis, B. H., *J. Catal.* **129**, 257 (1991).
14. Hobson, M. C., Goresh, S. L., Jr., and Khare, G. P., *J. Catal.* **142**, 641 (1993).
15. Li, Y. X., Klabunde, K. J., and Davis, B. H., *J. Catal.* **128**, 1 (1991).
16. Srinivasan, R., De Angeles, R. J., and Davis, B. H., *J. Catal.* **106**, 449 (1987).
17. Alerasool, S., Boecker, D., Rejai, B., Gonzalez, R. D., Del Angel, G., Asomoza, M., and Gómez, R., *Langmuir* **4**, 1083 (1988).
18. Del Angel, G., Medina, C., Gómez, R., Rejai, B., and Gonzalez, R., *Catal. Today* **5**, 395 (1989).
19. Rogemond, E., Essayem, N., Frety, R., Perrichon, V., Primet, M., and Mathis, F., *J. Catal.* **166**, 229 (1997).
20. De Menorval, L. C., Chaqroune, A., Coq, B., and Figueras, F., *J. Chem. Soc., Faraday Trans.* **93(20)**, 3715 (1997).
21. Queau, R., Labroue, D., and Poilblanc, R., *J. Catal.* **69**, 249 (1981).
22. Kili, K., and Le Normand, F., *J. Mol. Catal.* **140**, 267 (1999).
23. Fajardie, F., Tempere, J. F., Djega-Mariadassou, G., and Blanchard, G., *J. Catal.* **163**, 77 (1996).
24. Irving. R. J., and Magnusson, E. A., *J. Chem. Soc.* 2283 (1958).
25. Primet, M., Basset, J. M., Mathieu, M. V., and Prettre, M., *J. Catal.* **29**, 231 (1973).
26. Gómez, R., Bertin, B., López, T., Schifter, I., and Ferrat, G., *J. Mol. Catal.* **109**, 55 (1996).